

Preprint MPIH-V11-1999

On technically solving an effective QCD-Hamiltonian

Susanne Bielefeld, Jan Ihmels^a, and Hans-Christian Pauli

Max-Planck-Institut für Kernphysik, Heidelberg. e-mail: S.Bielefeld@mpi-hd.mpg.de

06 april 1999

Abstract. By their very nature, field-theoretical Hamiltonians are derived in momentum representation. To solve the corresponding integro-differential equations is more difficult than to solve the simpler differential equations in configuration space ('Schrödinger equation'). For the latter many different and very effective methods have been developed in the past. But rather than to Fourier-transform to configuration space – which is not always easy – the equations are solved here directly in momentum space, by using Gaussian quadratures. Special attention is given to the case where the potential in configuration space is linear and where the corresponding momentum-space kernel has an almost intractable $1/(\mathbf{k} - \mathbf{k}')^4$ -singularity. Its regularization requires a certain technical effort, introducing suitable counter terms. The method is numerically reliable and fast, faster than other methods in the literature. It should be useful to and also applicable in other approaches, including phenomenological Schrödinger-type equations.

PACS. 11.10.Ef Lagrangian and Hamiltonian approach – 11.15.Tk Other non-perturbative techniques – 12.38.Aw General properties of QCD (dynamics, confinement, etc.) – 12.38.Lg Other nonperturbative calculations

1 Introduction

Dirac's front form of Hamiltonian dynamics [1] seems to be a good candidate for addressing the thus far unsolved bound-state problem of a (gauge) field theory, particularly of non-Abelian quantum chromo-dynamics (QCD), as reviewed recently in [2]. Advantages are its comparatively simple vacuum structure and the simple boost properties. In fact, one can formulate the bound-state problem frame-independently, and if one uses the light-cone gauge $A^+ = 0$, the vacuum is trivial. More recently [3], the front-form Hamiltonian for QCD has been reduced to a renormalized, effective Hamiltonian which acts only in the Fock space of one quark (q) and one anti-quark (\bar{q}). One then faces the numerical problem to solve these equations.

In principle, one could proceed like in [4,5] for QED. But we prefer to move on slowly, by first suppressing in Section 2 all fine and hyperfine interactions with a simple trick. The resulting spin-less equation finds its analogue in the 'central potential' of a Schrödinger equation. In Section 3, the so truncated effective interaction is shown to interpolate smoothly – as a function of only one numerical parameter – between a pure Coulomb and a linear potential. These potentials in configuration space are presented

in detail, together with the known analytical solutions to the Coulomb and the linear potential. Their knowledge is advantageous to check the numerical procedures.

In Section 4 the counter term technology is presented in detail, and applied in Sections 5 and 6 to the Coulomb and the Yukawa, and in Section 7 to the combined problem, respectively. The respective eigenvalues and eigenfunctions are presented in all detail. More and perhaps redundant numerical results are compiled in the Appendix. A summary and a discussion in Section 8 rounds-off the paper.

2 The light-cone momentum-space approach

The front-form Hamiltonian for QCD has been reduced in [3] to an effective Hamiltonian, with a resulting integral equation in momentum space

$$\begin{aligned}
 & M^2 \langle x, \mathbf{k}_\perp; \lambda_q, \lambda_{\bar{q}} | \psi \rangle \\
 &= \left[\frac{\bar{m}_q^2 + \mathbf{k}_\perp^2}{x} + \frac{\bar{m}_{\bar{q}}^2 + \mathbf{k}_\perp^2}{1-x} \right] \langle x, \mathbf{k}_\perp; \lambda_q, \lambda_{\bar{q}} | \psi \rangle \\
 & - \frac{1}{3\pi^2} \sum_{\lambda'_q, \lambda'_{\bar{q}}} \int \frac{dx' d^2 \mathbf{k}'_\perp}{\sqrt{x(1-x)x'(1-x')}} \frac{\bar{\alpha}(Q)}{Q^2} \\
 & \langle \lambda_q, \lambda_{\bar{q}} | S(Q) | \lambda'_q, \lambda'_{\bar{q}} \rangle \langle x', \mathbf{k}'_\perp; \lambda'_q, \lambda'_{\bar{q}} | \psi \rangle . \quad (1)
 \end{aligned}$$

Send offprint requests to: Prof. H.C. Pauli, MPI für Kernphysik, Postfach 10 39 80, D-69029 Heidelberg. , archive: hep-th/9900xxx

^a now: Pembroke College, Cambridge CB21RF

The spectrum of the invariant-mass squared eigenvalues M^2 is the goal we want to reach. The corresponding eigenfunctions $|\psi\rangle$ are the probability amplitudes for finding a quark with longitudinal momentum fraction x , transversal momentum \mathbf{k}_\perp , and helicity λ_q , and correspondingly for the anti-quark. The physical (renormalized) masses of the quarks are denoted by \overline{m}_q . The 4-momentum transfer along the quark line $Q_q^2 = -(k - k')^\mu (k - k')_\mu$ is generally different from $Q_{\bar{q}}^2$. Their mean $Q^2 = (Q_q^2 + Q_{\bar{q}}^2)/2$ appears in Eq.(1). The (renormalized) ‘running’ coupling constant $\overline{\alpha}(Q)$ is a function of the momentum transfer and will be given below. The spinor factor

$$\begin{aligned} & (\lambda_q, \lambda_{\bar{q}} | S(Q) | \lambda'_q, \lambda'_{\bar{q}}) \\ & = [\overline{u}(k_q, \lambda_q) \gamma^\mu u(k'_q, \lambda'_q)] [\overline{v}(k_{\bar{q}}, \lambda_{\bar{q}}) \gamma_\mu v(k'_{\bar{q}}, \lambda'_{\bar{q}})] \end{aligned} \quad (2)$$

represents the current-current coupling and describes all fine and hyperfine interactions.

To reduce the complexity of the problem we introduce several simplifications and approximations, as follows. First, we suppress all fine and hyperfine interactions by setting

$$\begin{aligned} & [\overline{u}(k_q, \lambda_q) \gamma^\mu u(k'_q, \lambda'_q)] [\overline{v}(k_{\bar{q}}, \lambda_{\bar{q}}) \gamma_\mu v(k'_{\bar{q}}, \lambda'_{\bar{q}})] \Big|_{x=\frac{1}{2}; \mathbf{k}_\perp=0} \\ & \simeq 4\overline{m}_q \overline{m}_{\bar{q}} \delta_{\lambda_q \lambda'_q} \delta_{\lambda_{\bar{q}} \lambda'_{\bar{q}}} \end{aligned} \quad (3)$$

The helicity summations in Eq.(1) therefore drop out, and with equal quark masses $\overline{m}_q = \overline{m}_{\bar{q}} = m$ the equation simplifies to

$$\begin{aligned} M^2 \psi(x, \mathbf{k}_\perp) & = \frac{m^2 + \mathbf{k}_\perp^2}{x(1-x)} \psi(x, \mathbf{k}_\perp) \\ & - \frac{m^2}{\pi^2} \int \frac{dx' d^2 \mathbf{k}'_\perp}{\sqrt{x(1-x)x'(1-x')}} \psi(x', \mathbf{k}'_\perp) \frac{4}{3} \frac{\overline{\alpha}(Q)}{Q^2} \end{aligned} \quad (4)$$

The longitudinal momentum fraction ($0 \leq x \leq 1$) and the transversal momentum ($-\infty \leq k_{\perp,x} \leq \infty$) have different domains of integration. It is convenient [4,5] to transform integration variables $(x, \mathbf{k}_\perp) \rightarrow (k_z, \mathbf{k}_\perp)$ by

$$x = x(k_z) = \frac{1}{2} \left(1 + \frac{k_z}{\sqrt{m^2 + \mathbf{k}_\perp^2 + k_z^2}} \right) \quad (5)$$

All components of the ‘vector’ $\mathbf{k} = (k_z, \mathbf{k}_\perp)$ have then the same domain. The corresponding Jacobian is

$$\frac{dx}{x(1-x)} = \frac{2}{m} \frac{dk_z}{A^2(x, \mathbf{k}_\perp)} \quad (6)$$

with the A -factor defined by

$$m^2 A^4(x, \mathbf{k}_\perp) = \frac{m^2 + \mathbf{k}_\perp^2}{4x(1-x)} = m^2 + \mathbf{k}_\perp^2 + k_z^2 \quad (7)$$

The wave function ψ can always be substituted by an other function ϕ ,

$$\psi(x, \mathbf{k}_\perp) = \frac{A(x, \mathbf{k}_\perp)}{\sqrt{x(1-x)}} \phi(x, \mathbf{k}_\perp) \quad (8)$$

Replacing the invariant mass-square eigenvalue M^2 by the binding energy E , *i.e.*

$$M^2 = 4m^2 + 4mE \quad (9)$$

the original integral equation Eq.(1) becomes finally

$$\left[E - \frac{\mathbf{k}^2}{m} \right] \phi(\mathbf{k}) = -\frac{1}{2\pi^2} \int \frac{d^3 \mathbf{k}'}{A(\mathbf{k})A(\mathbf{k}')} \frac{4}{3} \frac{\overline{\alpha}(Q)}{Q^2} \phi(\mathbf{k}') \quad (10)$$

Note that the only approximation is the suppression of the fine and hyperfine interaction by Eq.(3).

At this point it is completely irrelevant that the equation holds actually for the front form. One simply does not recognize its origin. It could be an equation in the instant form, where only the (usual) three momenta \mathbf{k} play the role of integration variables. It would however not be trivial to Fourier transform this equation to configuration space, the factor A is preventing us to do that in a standard way. We therefore apply one further approximation. Somewhat doubtfully, we apply the non-relativistic approximation under the integral, and set

$$A(\mathbf{k}) \simeq A(\mathbf{k}') = 1, \quad Q^2 = (\mathbf{k} - \mathbf{k}')^2 \quad (11)$$

One now has a complete analogy with the simpler spinless case of an average potential. One could argue in favor of this approximation, that it is only consistent with Eq.(3). By replacing the QCD running coupling $4/3 \overline{\alpha}(Q)$ with the (physical) QED coupling α one obtains the usual Coulomb-Schrödinger equation in momentum space.

Amazingly enough, just by redefining the wave functions, we have derived an equation whose kernel is manifestly rotationally invariant. This is surprising since rotations perpendicular to the z -axis are dynamic operators in the front form and very complicated [2].

What shall be used for the effective coupling constant $\overline{\alpha}(Q)$? In [3] an explicit expression was given, but here we use the simplified expression of Brodsky *et al.* [7]

$$\overline{\alpha}(Q) = \frac{12\pi}{25 \ln \left[\frac{\mu^2 + Q^2}{\kappa^2} \right]} = \frac{12\pi}{25 \ln \frac{\mu^2}{\kappa^2} + 25 \ln \left[1 + \frac{Q^2}{\mu^2} \right]} \quad (12)$$

and adopt their numerical values

$$\kappa \simeq 160 \text{ MeV}, \quad \mu \simeq 872 \text{ MeV} \quad (13)$$

Now the problem is set.

Approximating the logarithm $\ln(1 + Q^2/\mu^2)$ by Q^2/μ^2 we parameterize the kernel of integral equation (10) as

$$\frac{4}{3} \frac{\overline{\alpha}(Q)}{Q^2} = \frac{2s^2}{(\mathbf{k} - \mathbf{k}')^2 (c^2 + (\mathbf{k} - \mathbf{k}')^2)} \quad (14)$$

With the parameter values of Eq.(13) one has

$$s = 1070 \text{ MeV}, \quad c = 1605 \text{ MeV} \quad (15)$$

Note that for $c \rightarrow 0$, the coupling constant in Eq.(14) exposes a $1/(\mathbf{k} - \mathbf{k}')^4$ singularity.

3 The potential in configuration space

Before solving numerically the equation

$$\left[E - \frac{\mathbf{k}^2}{m} \right] \phi(\mathbf{k}) = -\frac{s^2}{\pi^2} \int d^3\mathbf{k}' \frac{1}{Q^2(Q^2 + c^2)} \phi(\mathbf{k}') \quad (16)$$

with $Q^2 = (\mathbf{k} - \mathbf{k}')^2$,

we discuss its structure by transformation to configuration space. Applying the Fourier transformations according to

$$\begin{aligned} \psi(\mathbf{x}) &= \int d^3\mathbf{k} e^{i\mathbf{k}\mathbf{x}} \phi(\mathbf{k}), \\ V(\mathbf{x}) &= \int d^3\mathbf{q} e^{i\mathbf{q}\mathbf{x}} U(\mathbf{k}, \mathbf{k}'), \\ U(\mathbf{k}, \mathbf{k}') &\equiv -\frac{s^2}{\pi^2} \frac{1}{(\mathbf{k} - \mathbf{k}')^2 ((\mathbf{k} - \mathbf{k}')^2 + c^2)}, \end{aligned} \quad (17)$$

one obtains a Schrödinger equation

$$\left[E + \frac{\nabla^2}{2m_r} \right] \psi(\mathbf{x}) = V(\mathbf{x}) \psi(\mathbf{x}), \quad (18)$$

with the reduced mass $m_r = m/2$. The simple structure is a consequence of the kernel $U(\mathbf{k}, \mathbf{k}')$ depending only on the difference $\mathbf{k} - \mathbf{k}'$. Since $\int d^3\mathbf{q} e^{i\mathbf{q}\mathbf{x}} 1/(Q^2 + c^2) = -2\pi^2 e^{-cr}/r$, with $r = |\mathbf{x}|$, one has

$$V(\mathbf{x}) = \frac{\beta}{r} [e^{-cr} - 1] \quad (19)$$

where $\beta = 2s^2/c^2$ is similar to the usual fine-structure constant. The potential is a superposition of a Coulomb and a Yukawa potential, as visualized in Figs. 1 and 2. The behavior

$$V(|\mathbf{x}|) = \begin{cases} -\frac{2s^2}{c^2} + s^2 r & \text{for } r \rightarrow 0, \\ -\frac{2s^2}{c^2} \frac{1}{r} & \text{for } r \rightarrow \infty, \end{cases} \quad (20)$$

can be observed in the figures: For sufficiently small distances the potential is linear (up to an additional constant), and for large r it becomes a Coulomb potential. For either of these extremes the analytic solutions are known.

The eigenvalue E used in Eq.(16) depends on the three parameters m , s , and c . It is easy to show that it depends on them in the dimensionless combination

$$\eta = \frac{c^3}{ms^2} = \frac{2}{\beta} \frac{c}{m}. \quad (21)$$

By introducing the dimensionless variables

$$p = \frac{k}{m_r \beta}, \quad q^2 = \frac{Q^2}{m_r^2 \beta^2}, \quad \epsilon = \frac{2E}{m_r \beta^2} \quad (22)$$

we obtain

$$[\epsilon - p^2] \phi(p) = -\frac{1}{\pi^2} \int d^3p' \left[\frac{1}{q^2} - \frac{1}{q^2 + \eta^2} \right] \phi(p') \quad (23)$$

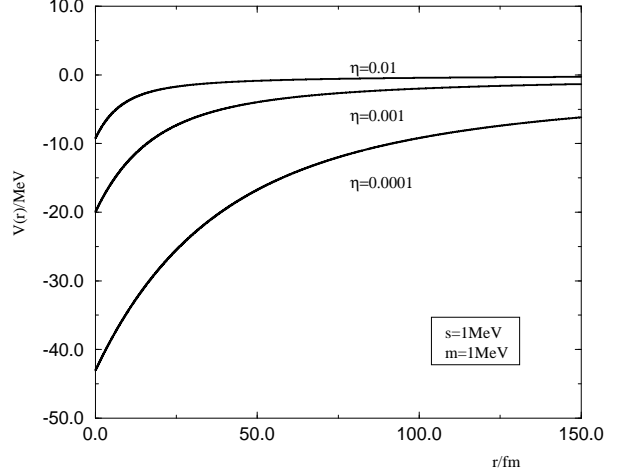


Fig. 1. The potential $V(r)$ is plotted versus r for different values of $\eta = 2c/\beta m$.— Note that for $r \rightarrow 0$ the potential goes to the finite value $-2s^2/c$, with a linear slope.

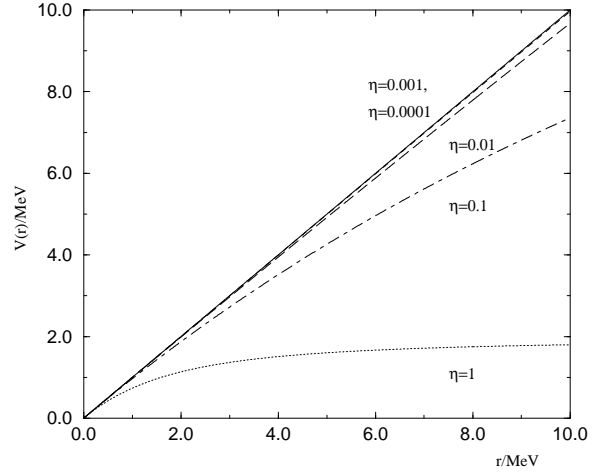


Fig. 2. Same as Fig. 1, but with the potential normalized to $V(0) = 0$.

which is much simpler than Eq.(16), and we will therefore focus on this version.

It has the two solvable limiting cases: (1.) For $\eta \rightarrow \infty$, the equation essentially shows the q^{-2} singularity of a Coulomb problem. (2.) For $\eta \rightarrow 0$, the equation has a q^{-4} singularity corresponding to a linear potential, whose eigenfunctions are the Airy functions.

The eigenvalues for the Coulomb problem are thus in our units

$$\epsilon_n = -\frac{1}{n^2}, \quad n = 1, 2, \dots \quad (24)$$

The eigenvalues for the linear potential are

$$\epsilon_n = -2\eta + \xi_n \eta^{\frac{4}{3}}, \quad n = 1, 2, \dots \quad (25)$$

where ξ_n are the zeros of the Airy functions $Ai(\xi_n) = 0$.

The knowledge of these two limiting cases is very useful for testing the numerical results.

4 Numerical solutions by Gaussian quadratures

Eq.(23) is an integral equation in the three variables \mathbf{p} . Restricting to s-waves one can integrate out the angles, which leads to an equation in one variable $p = |\mathbf{p}|$, *i.e.*

$$[\epsilon - p^2] \phi(p) = \frac{1}{\pi} \int_0^\infty dp' \frac{p'}{p} \left[\ln \frac{(p-p')^2}{(p+p')^2} - \ln \frac{(p-p')^2 + \eta^2}{(p+p')^2 + \eta^2} \right] \phi(p'). \quad (26)$$

It is convenient [9], to convert this integral equation for the unknown function $\phi(p)$ to a matrix equation for the unknown numbers $u_i \equiv \sqrt{\omega_i} \phi_i$ with $\phi_i \equiv \phi(p_i)$,

$$(p_i^2 + a_{ii}) u_i + \sum_{j \neq i} a_{ij} u_j = \epsilon u_i, \quad i, j = 1, \dots, N, \quad (27)$$

namely by approximating the integral with the finite sum of Gaussian quadratures,

$$\int_0^\infty f(p) dp \longrightarrow \sum_{i=1}^N \omega_i f(p_i). \quad (28)$$

The non-diagonal matrix elements are given by

$$a_{ij} = \frac{1}{\pi} \sqrt{\omega_i \omega_j} \frac{p_j}{p_i} \left[\ln \frac{(p_i - p_j)^2}{(p_i + p_j)^2} - \ln \frac{(p_i - p_j)^2 + \eta^2}{(p_i + p_j)^2 + \eta^2} \right]. \quad (29)$$

It is numerically convenient to map the infinite interval of Eq.(26) onto a finite one by transforming variables [10], according to

$$\int_0^\infty f(p) dp = \int_{-1}^1 f(p(y)) \frac{dp}{dy} dy. \quad (30)$$

The mapping function $y(p)$ is arbitrary, but must satisfy the boundary conditions

$$y(p=0) = -1, \quad y(p=\infty) = +1. \quad (31)$$

We choose

$$y(p) = 2e^{-\frac{p}{z}} - 1, \quad (32)$$

with an adjustable 'stretching' parameter z . With $c(y) \equiv dp/dy$, the quadratures then become

$$\sum_i f(p_i) \omega_i = \sum_i f(y_i) c(y_i) \hat{\omega}_i, \quad (33)$$

i.e. the transformation changes the weights ω_i into $\omega_i \equiv c(y_i) \hat{\omega}_i$. Thus

$$p_i = -z \ln \frac{1+y_i}{2} \quad \text{and} \quad \omega_i = \hat{\omega}_i \frac{z}{1+y_i}, \quad (34)$$

where the $\hat{\omega}_i$ and y_i are the tabulated weights and abscissas for the interval $[-1, 1]$. Finally Eq.(29) can be solved by conventional matrix diagonalization methods.

Eq.(27) poses a problem: The diagonal matrix elements a_{ii} diverge logarithmically. Problems like these can be solved by the Nyström method - by the technique of counter terms - as to be discussed next [10]. In principle one adds and subtracts in Eq.(23) a diagonal term $F(p)\phi(p)$. The idea is that one of them is treated analytically and the other by Gaussian quadratures, such that the singularity in a_{ii} cancels.

The construction of suitable counter terms must be done separately for the Coulomb and the Yukawa part. Therefore we discuss these two cases in Sections 5 and 6 individually. In Section 7 we return to the full problem.

5 The Coulomb problem

The Coulomb problem in momentum space was treated by Wölz [10,4] as a numerical exercise and will be repeated briefly. In analogy to Eq.(26) we want to solve

$$[\epsilon - p^2] \phi(p) = \frac{1}{\pi} \int_0^\infty dp' \frac{p'}{p} \ln \left[\frac{(p-p')^2}{(p+p')^2} \right] \phi(p'). \quad (35)$$

Adding and subtracting the analytically integrable Coulomb counter term $F_C(p)\phi(p)$

$$F_C(\mathbf{p}) = \frac{1}{\pi^2} \int d^3 \mathbf{p}' \frac{1}{(\mathbf{p} - \mathbf{p}')^2} \frac{(1 + \mathbf{p}^2)^2}{(1 + \mathbf{p}'^2)^2} \quad (36)$$

$$= 1 + \mathbf{p}^2. \quad (37)$$

one arrives at

$$(\epsilon - p^2 + (1 + p^2)) \phi(p) = \frac{1}{\pi} \int_0^\infty dp' \frac{p'}{p} \ln \left[\frac{(p' - p)^2}{(p' + p)^2} \right] \left[\phi(p') - \frac{(1 + p^2)^2}{(1 + p'^2)^2} \phi(p) \right]. \quad (38)$$

For $p = p'$, the term in the square bracket vanishes, *i.e.* it is justified to restrict to $j \neq i$ in the summation over j on the r.h.s. of Eq.(27). The diagonal matrix elements then become

$$a_{ii} = -(1 + p_i^2) - \frac{1}{\pi} \sum_{j \neq i} \omega_j \frac{p_j}{p_i} \ln \frac{(p_i - p_j)^2 (1 + p_i^2)^2}{(p_i + p_j)^2 (1 + p_j^2)^2}. \quad (39)$$

The off-diagonal matrix-elements in Eq.(29) are not affected by this procedure

$$a_{ij} = \frac{1}{\pi} \sqrt{\omega_i \omega_j} \frac{p_j}{p_i} \ln \frac{(p_i - p_j)^2}{(p_i + p_j)^2}, \quad (40)$$

see Eq.(29). In the sequel we ask ourselves whether this results can be improved by a stretching factor z , as given

n	Exact	Calculated					
		N=16			N=32		
		z = 0.70			z = 1.0		
1	-1.0000	-1.0000	-1.0000	-1.0000	-1.0000	-1.0000	-1.0000
2	-0.2500	-0.2545	-0.2525	-0.2516	-0.2523	-0.2510	-0.2506
3	-0.1111	-0.1160	-0.1135	-0.1126	-0.1145	-0.1122	-0.1117
4	-0.0625	-0.0683	-0.0649	-0.0639	-0.0676	-0.0637	-0.0630
5	-0.0400	-0.0471	-0.0425	-0.0414	-0.0485	-0.0415	-0.0406

Table 1. The eigenvalues of the Coulomb problem for two values of the stretching factor z and three matrix dimensions N are compared with the exact values.

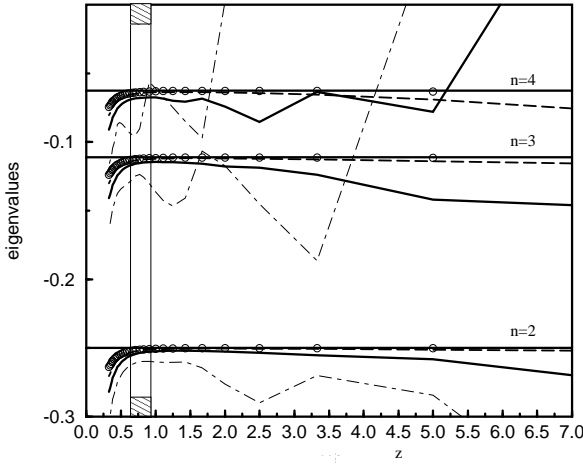


Fig. 3. The Bohr eigenvalues for $n = 2, 3, 4$ are plotted versus the stretching factor z for different matrix dimensions N (--- $N=8$, — $N=16$, - - - $N=32$ and \circ $N=64$). The exact eigenvalues $-1/n^2$ are shown as well. Note the hatched area, in which the numerical results are particularly stable against the number z .

in Eq.(34). The advantage of the stretching factor is that a particular choice shifts the bulk of integration points to the region where the wave function is significantly different from zero. In Fig. 3 the numerical eigenvalues of Eq.(27) with the matrix elements of Eqs.(39) and (40) are plotted versus z for different matrix dimensions N . As seen in the figure, the functions $\epsilon_n(z)$ are rapidly varying (almost fluctuating) for low dimensionality and become flatter with increasing N . For a z within the hatched area, however, the numerical results are rather stable as function of N . A value of $N = 32$ (or 16) seems to satisfy all practical requirements. The lowest eigenvalue ($\epsilon_1 = -1.0$) is not shown, since the function ($\epsilon_1(z)$) is completely flat. These observations are somewhat more quantified in Table 1.

The final results for the low lying part of the spectrum are accumulated in Fig. 4. The spectrum is remarkably insensitive to the matrix dimensions N . Also the numerical wave function as displayed in Fig. 5 is highly accurate. For all practical needs $N = 16$ is sufficient, see also Table 1.

One concludes that the particular choice of the stretching factor ($z = 0.70$) can be important for improving

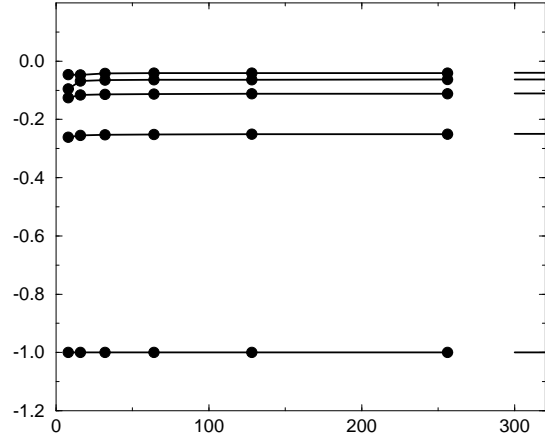


Fig. 4. The numerical eigenvalues for the Coulomb problem are plotted versus the number of integration points N (8, 16, 32, 64, 128, 256) for $z = 0.70$.

the rate of convergence and the precision of the Gaussian method for solving equations in momentum space.

6 The Yukawa potential

The Yukawa potential in momentum space obeys the integral equation

$$[\epsilon - p^2] \phi(p) = \frac{1}{\pi} \int_0^\infty dp' \frac{p'}{p} \ln \left[\frac{(p-p')^2 + \eta^2}{(p+p')^2 + \eta^2} \right] \phi(p'). \quad (41)$$

In analogy to the Coulomb problem, one adds and subtracts an analytically integrable counter term $F_Y(p)\phi(p)$

$$F_Y(\mathbf{p}) = \frac{1}{\pi^2} \int d^3 \mathbf{p}' \frac{1}{(\mathbf{p} - \mathbf{p}')^2 + \eta^2} \frac{(1 + \mathbf{p}^2)^2}{(1 + \mathbf{p}'^2)^2} \quad (42)$$

$$= \frac{(1 + \mathbf{p}^2)^2 (\mathbf{p}^2 + (\eta - 1)^2)}{(\mathbf{p}^2 + \eta^2 - 1)^2 + 4\mathbf{p}^2}.$$

The integral equation (41) is then rewritten as

$$\left(\epsilon - p^2 + \frac{(1 + p^2)^2 (p^2 + (\eta - 1)^2)}{(p^2 + \eta^2 - 1)^2 + 4p^2} \right) \phi(p) =$$

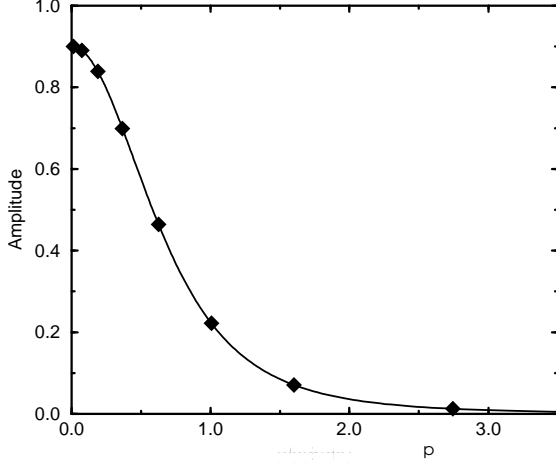


Fig. 5. The exact wave function $\phi(p_i)_{1s}$ for the Coulomb problem is plotted versus p (the momentum in units of the Bohr momentum), and compared with the numerical values $u_i\sqrt{4\pi\omega_i}$ (filled diamonds). Parameter values are $z = 0.70$ and $N = 8$.- Note the excellent agreement.

$$\frac{1}{\pi} \int_0^\infty dp' \frac{p'}{p} \ln \left[\frac{(p' - p)^2 + \eta^2}{(p' + p)^2 + \eta^2} \right] \quad (43)$$

$$\times \left[\phi(p') - \frac{(1 + p^2)^2}{(1 + p'^2)^2} \phi(p) \right].$$

The matrix equation (27) has then the diagonal elements

$$a_{ii} = -\frac{(p_i^2 + (\eta - 1)^2)(1 + p_i^2)^2}{(p_i^2 + \eta^2 - 1)^2 + 4p_i^2} \quad (44)$$

$$- \frac{1}{\pi} \sum_{j \neq i} \omega_j \frac{p_j}{p_i} \ln \left[\frac{(p_j - p_i)^2 + \eta^2}{(p_j + p_i)^2 + \eta^2} \right] \frac{(1 + p_i^2)^2}{(1 + p_j^2)^2},$$

while the off-diagonal elements are not modified

$$a_{ij} = \frac{1}{\pi} \sqrt{\omega_i \omega_j} \ln \frac{(p_j - p_i)^2 + \eta^2}{(p_j + p_i)^2 + \eta^2}. \quad (45)$$

The integral over the domain $[0, \infty]$ is mapped on the interval $[-1, 1]$ as given in Eqs.(30) to (34). The limit $\eta \rightarrow 0$ gives back the Coulomb problem, see Section 5. We have checked explicitly that the programs reproduce this case. A comparatively small value of η is $\eta = 0.01$. Indeed, the low lying part of the spectrum and the wave function is very similar to the corresponding result for the Coulomb problem in Figs. 4 and 5. In either case, the eigenvalues are practically insensitive to N , particular for the stretching parameter $z = 0.7$, chosen to be the same as for the Coulomb problem. One should note that the Yukawa problem has only a finite number of bound states. The value of $z = 1.25$ is obtained by the same optimalization procedure and shown explicitly in Fig. 6. Finally we summarize our best values for $\eta = 0.01$ and $\eta = 1.0$ in Table 2.

n	$\eta = 0.01$ $z = 0.7$	$\eta = 1.0$ $z = 1.25$
1	-0.8141	-0.0208
2	-0.1022	-0.0003
3	-0.0084	-
4	-0.0019	-
5	-0.0019	-

Table 2. The eigenvalues of all bounded s-states for the Yukawa problem for two values of η . The matrix dimension is either $N = 32$.

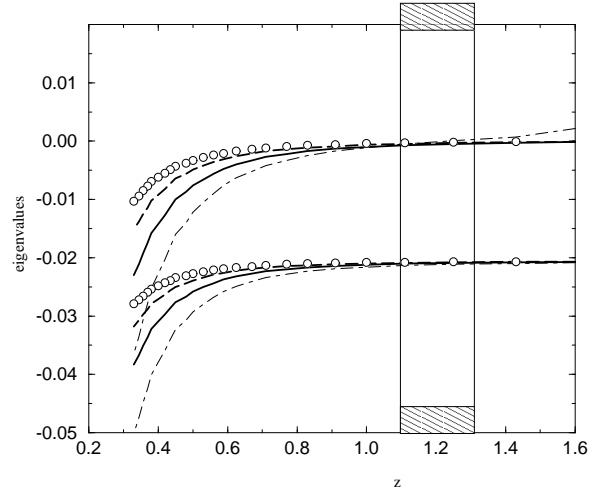


Fig. 6. The two lowest eigenvalues of the Yukawa problem with $\eta = 1.0$ are plotted versus the stretching factor z for different matrix dimensions: (--- N=8, — N=16, - - - N=32 and o N=64).

7 The hadronic Coulomb potential

Combining appropriately the considerations for the Coulomb and the Yukawa problem by adding and subtracting the counter terms $(F_C(p) + F_Y(p))\phi(p)$ as given in Sections 5 and 6, yield immediately the improved diagonal elements

$$a_{ii} = -(1 + p_i^2) + 2\eta + \frac{(p_i^2 + (\eta - 1)^2)(1 + p_i^2)^2}{(p_i^2 + \eta^2 - 1)^2 + 4p_i^2} \quad (46)$$

$$- \frac{(1 + p_i^2)^2}{\pi p_i} \sum_{j \neq i} \omega_j p_j \ln \left[\frac{(p_i - p_j)^2}{(p_i + p_j)^2} \right] \frac{1}{(1 + p_j^2)^2}$$

$$+ \frac{(1 + p_i^2)^2}{\pi p_i} \sum_{j \neq i} \omega_j p_j \ln \left[\frac{(p_j - p_i)^2 + \eta^2}{(p_j + p_i)^2 + \eta^2} \right] \frac{1}{(1 + p_j^2)^2},$$

which together with the unchanged off-diagonal elements a_{ij} as given in Eq.(29) define the matrix equation (27).

In the limit $\eta \rightarrow \infty$ the spectrum of Eq.(27) is expected to be very close to the Coulomb spectrum, $\epsilon_n = -1/n^2$, a fact, which has been used to test the computer codes. In Fig. 7 it is shown that the Coulomb limit is already well achieved for numerical values of $\eta \geq 2.0$.

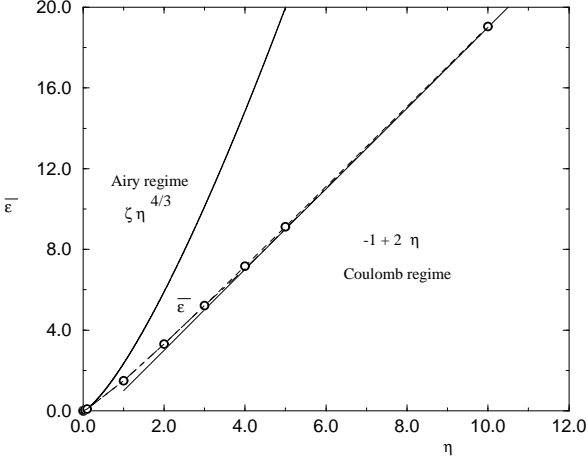


Fig. 7. The lowest eigenvalue $\bar{\epsilon}(\eta) = \epsilon + 2\eta$ is plotted versus η (\circ). The upper solid line indicates the Airy-type solution and the lower solid line visualizes the Coulomb-type solution.

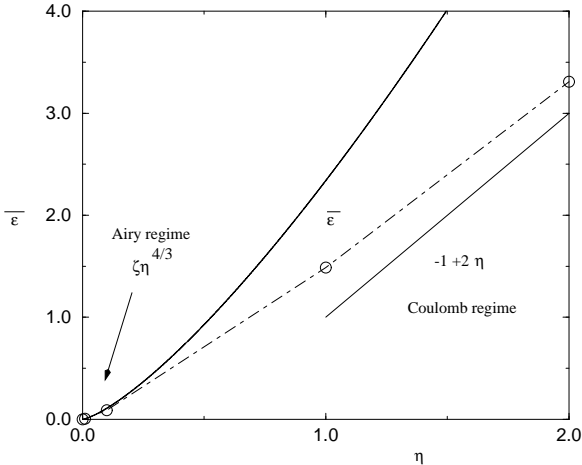


Fig. 8. A zoom of Fig. 7

In the other limit, $\eta \rightarrow 0$, the spectrum of Eqs.(26) or (27) is expected to approach the spectrum for a linear potential, *i.e.* $\epsilon_n = -2\eta + \xi_n \eta^{4/3}$. A typical Airy-solution, however, is achieved only for very small values, *i.e.* $\eta \leq 0.02$, as seen in Fig. 8.

For all other values, the spectrum is somehow intermediate between those two extreme cases, as quantitatively demonstrated in Table 3. It is remarkable how the curve of the calculated eigenvalues $\bar{\epsilon}(\eta) = 2\eta + \epsilon_1$ in Fig. 8 interpolates between the two asymptotic curves $\bar{\epsilon}(1) \sim \eta^{4/3}$ and $\bar{\epsilon}(1) \sim 2\eta - 1$.

Note that the stretching factor z should be optimized for each value of η . The resulting value is given in Table 3 as well. In parenthesis we note that the Coulomb limit for the present hadronic case is reachable for $\eta \rightarrow \infty$ while for the Yukawa case it was $\eta \rightarrow 0$ (see Section 6).

More explicit numerical results are given in App. A.

8 Summary and discussion

Since the components of total four-momentum commute with each other, a field theoretic Hamiltonian is formulated quite naturally in momentum representation. In the instant form (usual quantization) the constituent's degrees of freedom are the three space-like momenta (and their helicities and flavors), in the front form (or in light-cone quantization) they are the longitudinal momentum fraction x and the two transversal momenta \mathbf{k}_\perp . Effective Hamiltonians have the same property, they become integral equations in momentum space. Usually, one Fourier-transforms such a momentum-space integral equation to a Schrödinger-type equation in configuration space and solves it by the familiar methods. Taking Fourier transforms is however not always easy, if not impossible, without additional assumptions.

In the present work we therefore want to solve the integral equations directly in momentum space. In particular, we look at an integral equation with an interaction kernel like

$$U(\mathbf{k}, \mathbf{k}') = -\frac{s^2}{(\mathbf{k} - \mathbf{k}')^2 (c^2 + (\mathbf{k} - \mathbf{k}')^2)} \frac{1}{\pi^2}$$

as derived in Section 2. We want to calculate the eigenvalues and eigenfunctions for the full range of the interaction parameters s and c , and of the physical mass m of the constituent particles, a quark and an anti-quark with equal mass. As shown in Section 3 the solutions are a function of only one dimensionless parameter

$$\eta = \frac{c^3}{ms^2},$$

which intern can be interpreted as the ratio of two dimensionless parameters, c/m and s/c . The limit $\eta \rightarrow \infty$ corresponds to a pure-Coulomb kernel $U \simeq (\mathbf{k} - \mathbf{k}')^{-2}$, the limit $\eta \rightarrow 0$ generates the highly singular interaction kernel $U \simeq (\mathbf{k} - \mathbf{k}')^{-4}$, as typical for a linear potential. The latter case was also the topic of Hersbachs work [6].

As demonstrated in several examples in Section 7, the transitional region with $\eta \sim 1.0$ corresponds to a superposition of a Coulomb and a Yukawa potential, which both are studied on their own merit in Sections 5 and 6, respectively. Therefore, for values of s and c fixed by their default value in Eq.(15), the spectra for a mass larger than typically 180 GeV are more like those in a linear potential, as opposed to more Coulomb-like spectra for masses smaller than typically 1.8 GeV. Masses in between have led to a mixed pattern.

The technical problem of solving the interaction kernel in momentum space is approached by discretization via Gaussian quadratures, and diagonalization of the so generated Hamiltonian matrix. Much attention is paid to speed up convergence by a counter-term technology already developed for the pure Coulomb case [4,10]. It is summarized in Sections 4 and 5. In Sections 6 and 7 it

η	z	$\bar{\epsilon} = \epsilon + 2\eta$	Airy regime $\xi_1 \eta^{\frac{4}{3}}$	Coulomb regime $-1 + 2\eta$
0.001	0.0370	0.00021905	0.00023381	
0.01	0.0714	0.00454474	0.00503728	
0.1	0.2174	0.08860885	0.10852499	
1.0	0.3861	1.48676105	2.3381	1
2.0	0.4762	3.31000318		3
4.0	0.8000	7.16112492		7
10.0	0.8333	19.04647165		19

Table 3. The eigenvalues $\epsilon + 2\eta$ of the integral equation (26) are given for increasing analytical values of the physical parameter η , Column 2 gives the actual stretching parameter z . In the last two columns the corresponding eigenvalue for the Airy or Coulomb regime are quoted for purpose of comparison.

n	N=16	N=32	N=64	N=16	N=32	N=64
$\eta = 0.01, z = 0.0714$						
1	0.0045	0.0045	0.0046	0.0884	0.0886	0.0887
2	0.0073	0.0074	0.0075	0.1312	0.1316	0.1317
3	0.0092	0.0094	0.0095	0.1541	0.1548	0.1549
4	0.0106	0.0110	0.0110	0.1674	0.1685	0.1686
$\eta = 1.0, z = 0.3861$						
1	1.4860	1.4868	1.4871	19.0456	19.0465	19.0470
2	1.8183	1.8193	1.8196	19.7537	19.7551	19.7555
3	1.9090	1.9102	1.9105	19.8877	19.8898	19.8903
4	1.9447	1.9464	1.9468	19.9339	19.9372	19.9379
$\eta = 10.0, z = 0.833$						

Table 4. The spectrum $\epsilon_n + 2\eta$ for different values of η and N , at the optimized value of z .

is adapted to the Yukawa and the combined Yukawa plus Coulomb problem, in this work referred to as the hadronic Coulomb problem by obvious reasons. Special emphasis is put on a free formal parameter, called the stretching factor z , which can be adjusted for a considerably increased numerical precision and stability. This way, one can restrict – on the average – on matrix diagonalization problems with a matrix dimension as small as $N = 32$. This part of the technical problem is applicable to many other physical problems. The restriction to equal masses of the constituents can be relaxed easily.

We find it remarkable, that we solve a problem which on the technical level looks like a problem of usual (equal-usual-time) quantization despite the fact that the generated solutions hold for the front form. The equation actually being solved cannot be recognized as to have its roots in light-cone quantization. The only physical assumption entering the considerations in Section 2 is that the current-current term was replaced by the term of leading order in Eq.(3).

It is, of course, still a long way to go for solving an effective QCD Hamiltonian on the technical level. Only a few steps have been taken in the present work. On the long run, we want to include properly the non-local factors $A(\mathbf{k})$ in Eq.(10), to relax the assumption of Eq.(3), and to insert more general expressions for the effective coupling constant $\bar{\alpha}(Q)$. Work in this direction is under way.

1. P.A.M. Dirac, Rev. Mod. Phys. **21**, 392 (1949).
2. S.J. Brodsky, H.C. Pauli, and S.S. Pinsky, Physics Reports **301**, 299-488 (1998).
3. H.C. Pauli, Eur. Phys. J. **C7**, 289 - 303 (1999).
4. M. Krautgärtner, H.C. Pauli, and F. Wölz, Phys. Rev. **D45**, 3755 (1992).
5. U. Trittmann, hep-th/9808077, hep-th/9704215, hep-th/9705021, hep-th/9705072.
6. H. Hershbach, Phys. Rev. **D47**, 7 (1993).
7. S.J. Brodsky, C.R. Ji, A. Pang, and D.G. Robertson, hep-ph/9705221, Phys.Rev. **D57**, 245-252 (1998).
8. H.C. Pauli, preprint MPIH-V26-1997, hep-ph/9707361.
9. T. Eller and H.C. Pauli, Z. Phys. **C42**, 59 (1989).
10. F. Wölz, Diploma Thesis, Heidelberg, February 1990.

A Some selected numerical results

In this appendix we add a few typical results for the hadronic Coulomb potential as discussed in Section 7. The spectra and s-wave eigenfunctions for a very small and a large value of η are shown to illustrate the main differences. The structure of the spectrum for $\eta = 0.01$ is similar to those of a linear potential. With increasing values of η , the shape of the spectrum changes to that of a Coulomb potential particularly for the large value $\eta = 10.0$. More results are available from the authors on request.

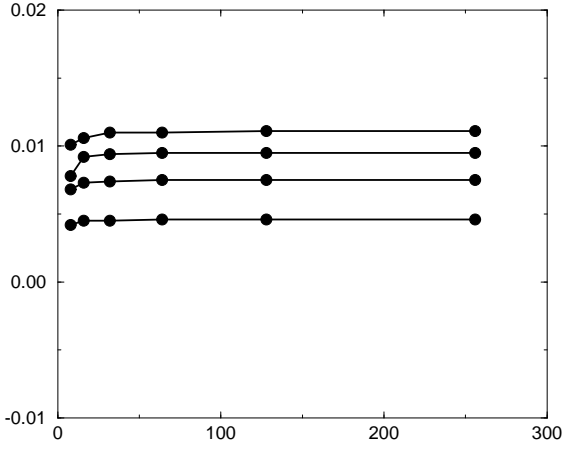


Fig. 9. The eigenvalues $\epsilon + 2\eta$ for $\eta = 0.01$ ($z = 0.0714$) are plotted versus the number of integration points N (8, 16, 32, 64, 128, 256).- Note the almost equidistant structure as in a linear potential.

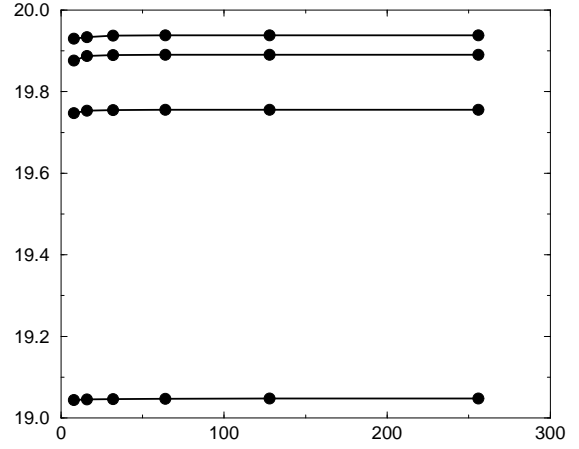


Fig. 11. The eigenvalues $\epsilon + 2\eta$ for $\eta = 10.0$ ($z = 0.833$) are plotted versus the same number of integration points as left.- This spectrum is of the Coulomb type, see Fig. 4.

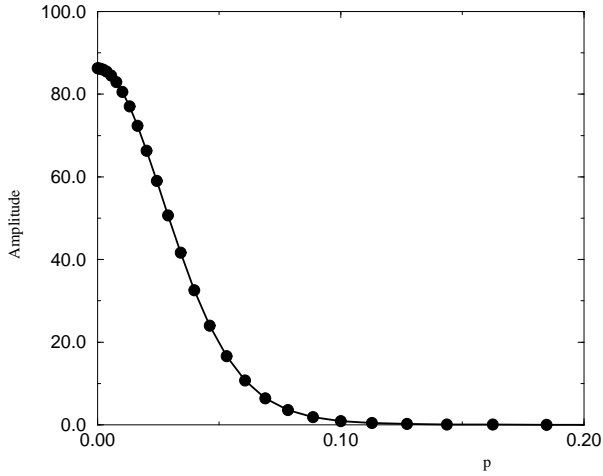


Fig. 10. The s-wave eigenfunction for $\eta = 0.01$ is plotted versus the momenta in Bohr units.- Note that the most of the integration points are in that region where the wave function is significantly different from zero. This is due to the choice of $z = 0.0714$.

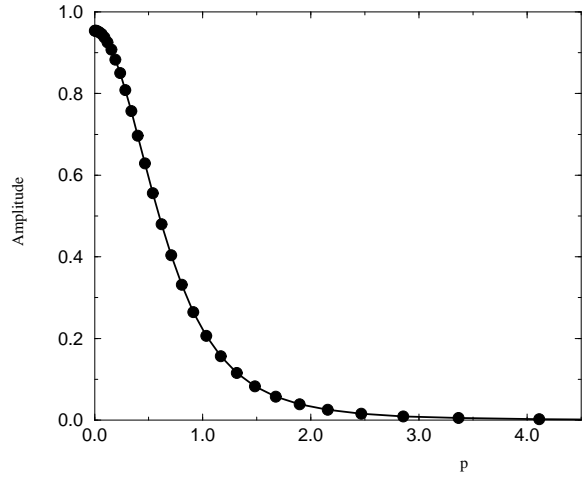


Fig. 12. The s-wave eigenfunction for $\eta = 10.0$ ($z = 0.833$) is plotted versus the momentum values p/p_{Bohr} .- This figure is comparable with Fig.5.

The following parts are not included in the printed work.

B Results for the Yukawa potential

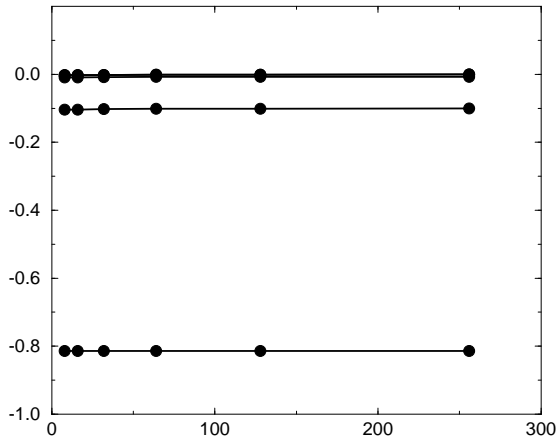


Fig. 13. Spectrum for $\eta = 0.01$

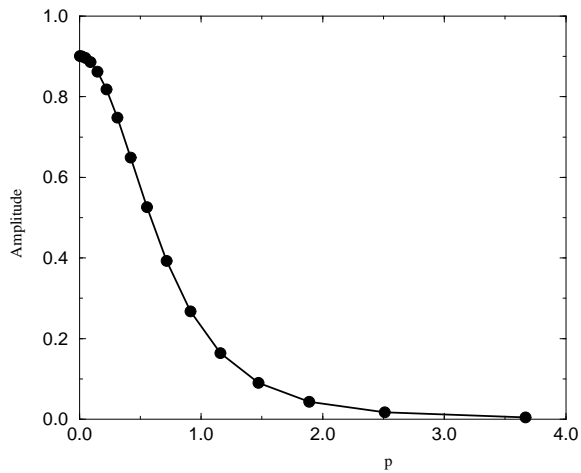


Fig. 14. S-wave eigenfunction for $\eta = 0.01$

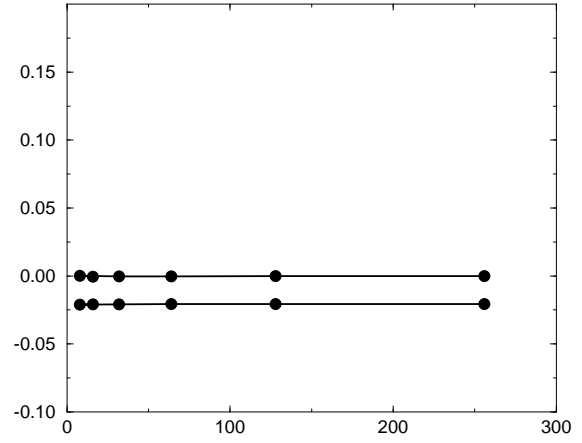


Fig. 15. Spectrum for $\eta = 1.0$

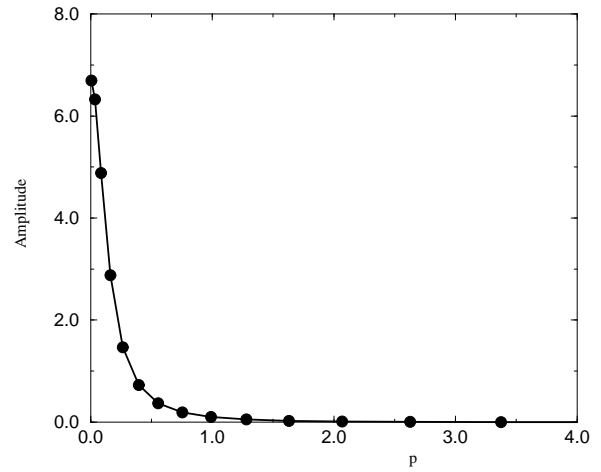


Fig. 16. S-wave eigenfunction for $\eta = 0.1$

C more numerical results for the hadronic Coulomb potential

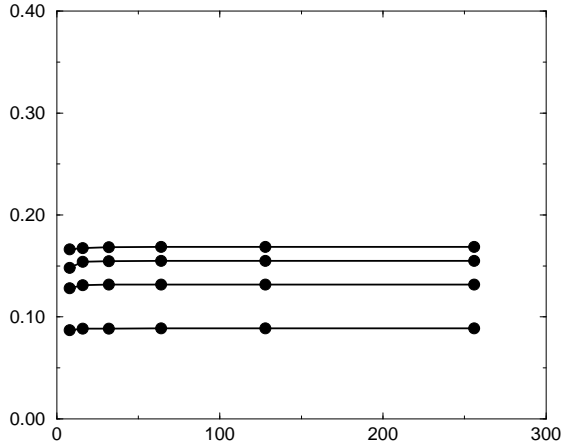


Fig. 17. Spectrum for $\eta = 0.01$

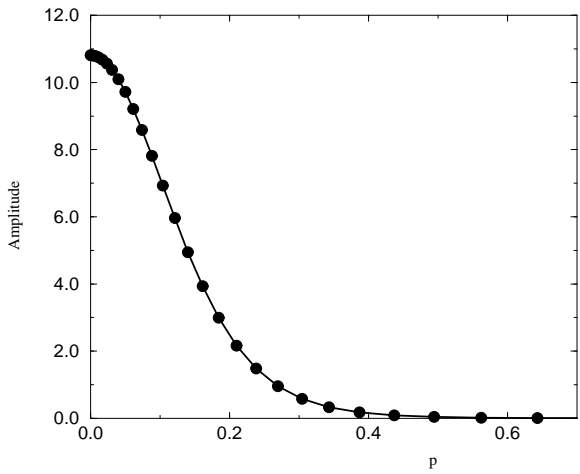


Fig. 18. S-wave eigenfunction for $\eta = 0.1$

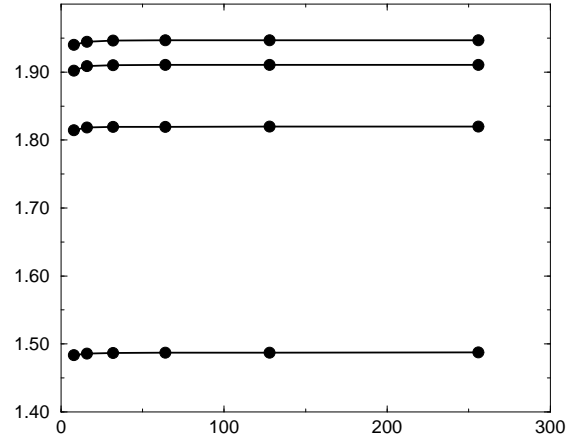


Fig. 19. Spectrum for $\eta = 1.0$

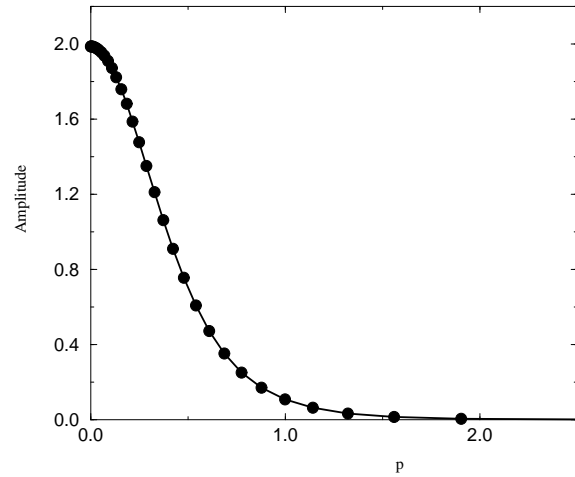


Fig. 20. S-wave eigenfunction for $\eta = 1.0$

D Determination of z for the hadronic Coulomb potential

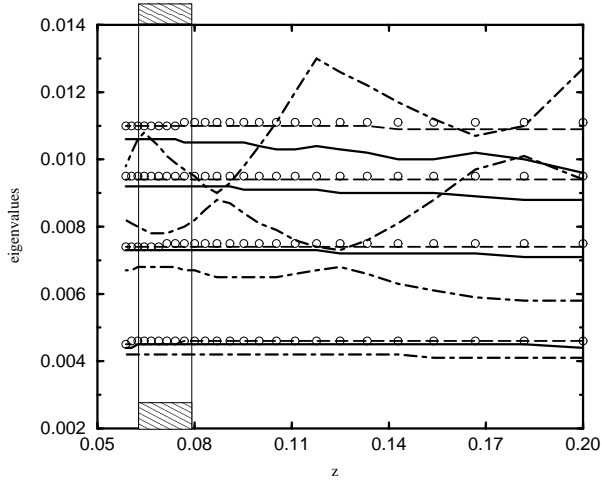


Fig. 21. Eigenvalues for $\eta = 0.01$ versus stretching z

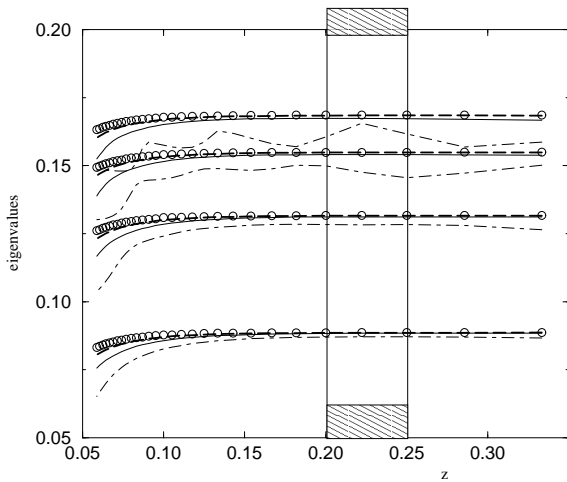


Fig. 22. Eigenvalues for $\eta = 0.1$ versus stretching z

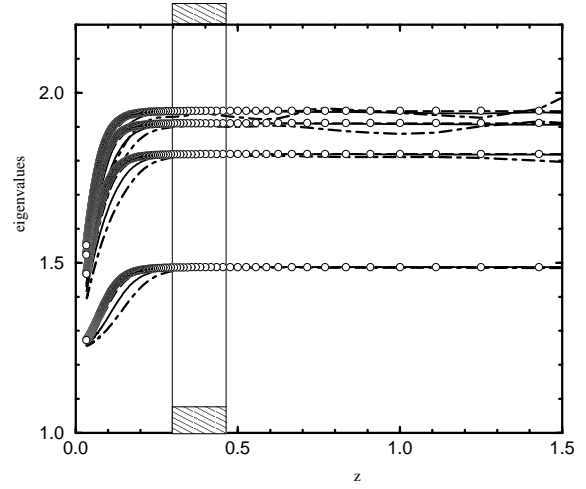


Fig. 23. Eigenvalues for $\eta = 1.0$ versus stretching z

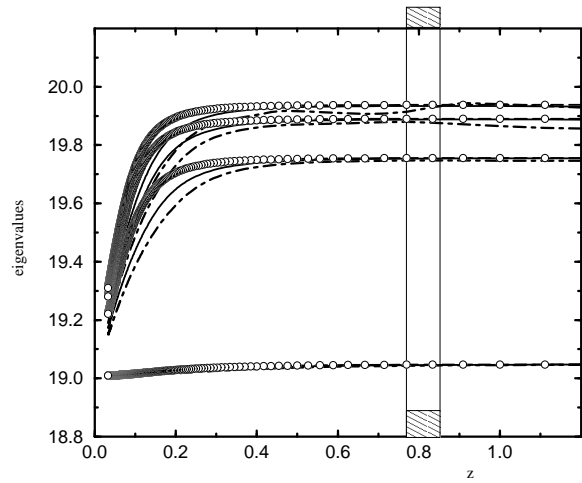


Fig. 24. Eigenvalues for $\eta = 10.0$ versus stretching z